Terahertz Rotational Spectroscopy of Greenhouse Gases Using Long Interaction Path-Lengths

Arnaud Cuisset, Francis Hindle, Gaël Mouret, Robin Bocquet, Jonas Bruckhuisen, Jean Decker, Anastasiia Pienkina, Cédric Bray, Éric Fertein, Vincent Boudon

MDPI

Article

Terahertz rotational spectroscopy of greenhouse gases using long interaction path-lengths

Arnaud Cuisset [1,*] 0000-0002-4358-2819, Francis Hindle[1] 0000-0001-9925-4497, Gaël Mouret[1] 0000-0002-8770-8188, Robin Bocquet[1] 0000-0002-7498-3527, Jonas Bruckhuisen [1] 0000-0002-0141-1034, Jean Decker[1] 0000-0003-3616-1570, Anastasiia Pienkina[1,2] 0000-0002-7249-8771, Cédric Bray[1,†], Éric Fertein[1] 0000-0001-9936-1700 and Vincent Boudon [3,*] 0000-0001-5015-6538

1 Université du Littoral Côte d'Opale, UR 4493, LPCA, Laboratoire de Physico-Chimie de l'Atmosphère, F-59140 Dunkerque, France; cuisset@univ-littoral.fr(A.C.); hindle@univ-littoral.fr(F.H.); mouret@univ-littoral.fr(G.M.); bocquet@univ-littoral.fr(R.B.); jonas.bruckhuisen@univ-littoral.fr(J.B.); jean.decker@univ-littoral.fr(J.D.); fertein@univ-littoral.fr(E.F.)
2 SATT-Nord, 25, Avenue Charles Saint-Venant, 59800 Lille, France; Anastasiia.Pienkina@sattnord.fr(A.P)
3 Laboratoire Interdisciplinaire Carnot de Bourgogne, UM 6303 CNRS, Université de Bourgogne Franche-Comté, 9 Av. A. Savary BP47870, F-21078, Dijon Cedex, France; vincent.boudon@u-bourgogne.fr(V.B.)
* Correspondence: cuisset@univ-littoral.fr(A.C.);vincent.boudon@u-bourgogne.fr(V.B.)
† Laboratoire Charles Coulomb, UMR 5221 CNRS, Université de Montpellier, Campus Triolet, Place Eugène Bataillon, F-34095 Montpellier Cedex 5, France; cedric.bray@umontpellier.fr(C.B.)

Version January 18, 2021 submitted to Appl. Sci.

Abstract: Even if on-board mm-wave/THz heterodyne receivers have been developed to measure greenhouse gases (GHGs) atmospheric profiles, rotational spectroscopy rests under-exploited for their monitoring unlike IR rovibrational spectroscopy. The present study deals with the ability of THz spectroscopy using long interaction path-lengths for GHG laboratory investigations. High-resolution THz signatures of non-polar greenhouse molecules may be observed by probing very weak centrifugal distortion induced rotational transitions. To illustrate, new measurements on CH_4 and CF_4 have been carried out. For CH_4, pure rotational transitions, recorded by cw-THz photomixing up to 2.6 THz in a White type cell adjusted to 20 m, have allowed to update the methane line list of atmospheric databases. Concerning CF_4, Fabry-Perot THz absorption spectroscopy with a km effective pathlength was required to detect line intensities lower than 10^{-27} cm^{-1}/(molec cm^{-2}). Contrary to previous synchrotron based FT-FIR measurements, the tetrahedral splitting of CF_4 THz lines is fully resolved. Finally, quantitative measurements of N_2O and O_3 gas traces have been performed in an atmospheric simulation chamber using a submm-wave amplified multiplier chain coupled to a Chernin type multi-pass cell on a 200 m path-length. The THz monitoring of these two polar GHGs at tropospheric and stratospheric concentrations may be now considered.

Keywords: *greenhouse gases; terahertz; long interaction path-lengths; rotational spectroscopy; trace gas monitoring.*

1. Introduction

The main discussion on climate change tends to focus on carbon dioxide (CO_2), the most dominant Greenhouse Gas (GHG) (65% of the global emission) produced by the burning of fossil fuels, industrial processes and changes in land use (deforestation, intensification of agriculture, flooding...) [1]. But CO_2 is not the only GHG driving the global climate change: methane (CH_4), nitrous oxide (N_2O), tropospheric ozone (O_3) and fluorinated gases have a direct contribution to the greenhouse effect. In

particular, the radiative forcing (warming influence) of long-lived GHGs such as tetrafluoromethane (CF_4) with a 50000 years lifetime in earth's atmosphere [2], is undergoing accelerating growth (almost a third of the increase attributed to the industrial age has been over the past 30 years) [3,4]. Several currently-operating satellite and air-borne missions aim to estimate emissions and absorptions of the main GHGs. By monitoring the column densities in our atmosphere, they accumulate new knowledge on their global distribution and temporal variation. Fourier Transform Spectrometers (FTS) are the most popular instruments used in these missions analysing the IR radiations reflected from the Earth's surface and emitted from the atmosphere and the surface. We can mention: (i) the IASI interferometer in the European MetOp satellite which monitors CO_2, O_3, CH_4, N_2O GHG column amounts in several IR channels of detection [5]; (ii) ACE on board the Canadian Satellite SCISAT where CF_4 and others CFCs/HCFCs are retrieved routinely in addition to the most abundant GHGs [6]; (iii) TES on board the Aura spacecraft which retrieves the O_3 and CH_4 profiles in the lower atmosphere from their rovibrational signatures [7]. Amongst the Aura's instruments, there is also a passive microwave limb-sounding (MLS) radiometer/spectrometer used to measure the pollution in the upper troposphere in the presence of ice clouds and volcanic aerosols, which prevent measurements by IR/UV techniques. The MLS instrument monitors O_3 and N_2O by measuring pure rotational lines in the mm-wave (240 GHz) and in the submm-wave (640 GHz) domains, respectively [8]. More recently, the National Space Science Center of the Chinese Academy of Sciences has developed a THz Atmospheric Limb Sounder (TALIS) for atmospheric vertical resolved profile observations: as for MLS/Aura, O_3 and N_2O are the targeted GHGs and their rotational transitions are probed with four heterodyne radiometers (LO frequencies: 118 GHz, 190 GHz, 240 GHz and 643 GHz) and several FFT spectrometers of 2 GHz bandwidth with 2 MHz resolution [9]. With this instrument, they are able to retrieve the N_2O and O_3 profiles with average precisions lower than 10 % and 5 % from 10 to 42 kms and from 10 to 70 kms altitude, respectively.

Accurate THz laboratory measurements are required in order to provide the best set of GHGs rotational line parameters (frequencies, widths, intensities…) and to optimize the inversion processes in GHGs atmospheric concentrations retrieval. The quality of the fits depends directly on the SNR of high resolution THz spectra and consequently on the sensitivity of the spectrometers [10]. According to the Beer-Lambert law, longer interaction THz path-lengths are required in the situation of a weak absorption. With longer wavelengths and larger beamsizes, the control of the propagation of THz radiations on long-range beam paths is challenging compared to that carried out in the IR/UV regions. Nevertheless, recent progress has allowed gas phase THz spectroscopy experiments with molecules/beam interaction distances from several tens to several hundreds of meters [11] to be performed. This article highlights recent advances of THz spectroscopy performed by our group, using long-interaction path-lengths for the measurement of weak GHG rotational absorptions. The ability to measure fully resolved centrifugally induced rotational transitions of non polar GHGs such as CH_4 and CF_4 will be demonstrated and the first THz measurements in an atmospheric simulation chamber will be presented towards the detection of polar stable N_2O and unstable O_3 GHGs at trace levels.

2. Materials and Methods

With the exception for the production of ozone, commercially available high purity CH_4, N_2O, and CF_4 GHGs with natural isotopic abundances were used throughout. The ozone was produced by corona discharge generation with pure oxygen (Air Tree Ozone Technology, C-Lasky C-L010-DTI). Various THz sources and detectors have been used in the studies presented here. In particular, three commonly used approaches, optical, optoelectronic and electronic, have been employed for the generation of the THz radiation.

2.1. Synchrotron based FT THz spectroscopy

The AILES beamline of the SOLEIL synchrotron was used for high-resolution broadband FT measurements in the 0.6 to 19.5 THz, (20-650 cm^{-1}) spectral range on CH_4 and CF_4. The very

bright light extracted from the synchrotron bending magnet has the advantage of displaying a lower divergence compared with other sources aiding its use with long path interaction White type cells. The FT IFS125 spectrometer, used in this case, has a 5 m delay stage allowing a resolution of 30 MHz to be achieved [17].

2.2. Cw-THz spectroscopy by photomixing

Alternatively higher resolution measurements can be made using monochromatic THz sources. The generation of THz radiation by photomixing is a frequency down-conversion technique which was used for the measurements of individual rotational lines of CH_4 up to 2.6 THz [12]. Two extended cavity laser diodes operating around 780 nm are mixed together in a LTG-GaAs device. The lasers are detuned to the desired THz frequency inducing a corresponding current in the photomixer device which is coupled to an integrated log spiral antenna [21]. The radiation is pre-colimated by a silicon hyper-hemispherical lens and propagated in free space. This type of source is monochromatic with excellent spectral purity and can be used in the range of 100 GHz to 3.3 THz. The available power is limited to 0.1 nW from 2.5 THz. By locking onto a frequency comb, the generated THz frequency is determined with a kHz accuracy [13]. Both amplitude and frequency modulation schemes can be easily implemented with this source, it does however suffer from available low power levels at the highest frequencies.

2.3. Submm-wave spectroscopy with amplified multiplier chains

We have used two AMC from the Virginia Diodes Inc. as electronic sources for the submm-wave measurements coupled to CHARME (see section 3.2) and to the THz FP cavity (see section 3.3). They are based on the up-conversion of a synthesized microwave frequency using a cascade of Schottky diode frequency multipliers mounted in rectangular wave-guide blocks. The guided radiation is launched into free space using a horn antenna and propagated through the interaction cell. Frequencies from 100 GHz to 1 THz can be conveniently produced and easily modulated in either amplitude or frequency as desired [27]. A typical power of 50 μW is available at 600 GHz.

2.4. Detection schemes

For all experiments, two types of detector have been employed. Zero Biased Detector (ZBD) is an unbiased Schottky diode mounted in a wave-guide operating in detection mode. This type of detector is uncooled and can provide a typical NEP of 10 $pW/\sqrt{Hz}$. When greater sensitivity was required a Helium cooled bolometer was used with a NEP of 1 $pW/\sqrt{Hz}$. For the measurements of very weakly intense CF_4 lines, we have coupled a very high finesse FP cavity with an AMC in order to reach very long equivalent interaction paths (see section 3.3). A control loop is used to lock the cavity to the frequency of the AMC with a frequency modulation providing an error signal. The second harmonic of the frequency modulation is simultaneously exploited to detect the presence of molecular absorption present in the cavity. The AMC frequency and cavity are thus swept together allowing sensitive absorption measurements to be made [34].

3. Results and discussion

3.1. THz measurements of CH_4 in a White type multi-pass cell

THz long-path spectroscopic experiments were initially conducted in the 2000's using home-made or commercial White type gas cells. The White cell was first described in 1942 by John U. White [14] and was a significant improvement over previous long path measurement techniques used in optical spectroscopy. A White cell is constructed using three spherical, concave mirrors having the same radius of curvature. The mirrors are separated by a distance equal to their radii of curvature. FT Michelson based interferometers have been connected by different groups to White type gas cells

allowing to improve the detection sensitivity in the Far-IR domain. The THz pathlengths reached vary from several tens of meters with classical sources such as Hg lamps [15,16] up to 180 m with weakly divergent and high brigthness Far-IR synchrotron radiations [17,18]. As example, the White type cell connected to the Bruker IFS125 high-resolution interferometer coupled to the AILES Far-IR/THz beamline of the SOLEIL synchrotron is shown in Fig. 1 (right part). Optoelectronic THz sources have been also coupled to White type cells to attempt THz rotational transitions measurements with long pathlengths (see Fig. 1, left part). Ppm and subppm LOD of strongly polar compounds were reached in pulsed THz-TDS and in cw-THz spectroscopy with maximal THz path-lengths of 5 m [20] and 20 m [21], respectively.

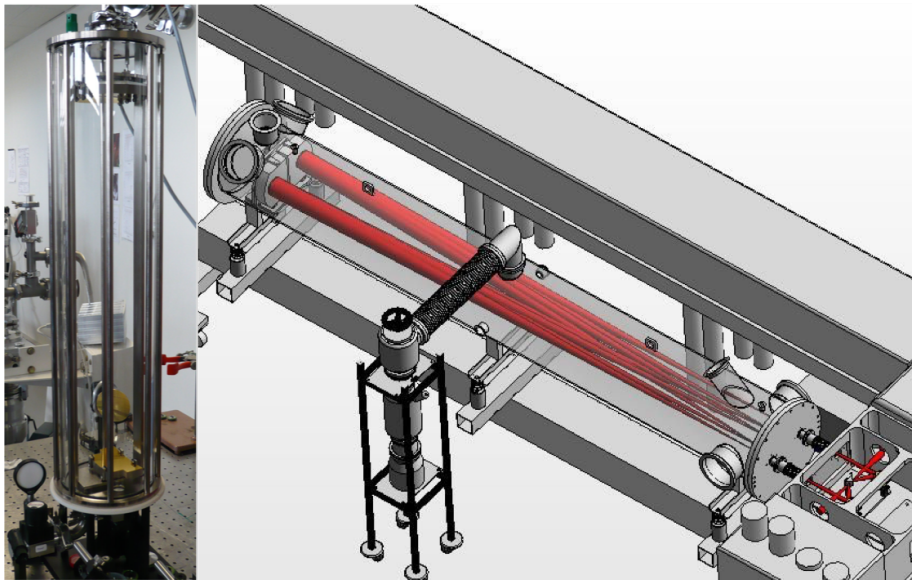

Figure 1. Picture/Scheme of the two White-type gas cells used for the CH_4 rotational spectra measurements. Left: standard White-type cell (Infrared Analysis, 35-V) used in the cw-THz photomixing measurement [21]. Right: White-type cell located in the AILES beamline of the SOLEIL synchrotron[17].

To date, the spectroscopic investigation of pure rotational THz transitions of CH_4 provides probably the best results in terms of sensitivity obtained by coupling cw-THz sources with White-type cells. Even if CH_4 is not polar, centrifugal distortion and vibrational effects induce a weak dipole ($\simeq$ 1 μD) which allows transitions between rotational energy levels. So very weak rotational absorptions in the THz domain may be measured with an optimized level of sensitivity. Using the HITRAN database and its graphical tool "HITRAN on the web" [22,23], the rotational absorbance of pure methane has been modelled in Fig. 2 (main panel) in the 2.0 - 2.7 THz frequency range for a THz path length of 20 m and a pressure of 10 mbar. The THz spectroscopy of CH_4 requires the measurements of very weak rotational absorptions lower than 2×10^{-5} cm^{-1} in a THz frequency region difficult to access. FT-Far-IR synchrotron based spectroscopy [18,19] and cw-THz by photomixing [12] succeeded to measure these weak rotational lines (see insets Fig. 2) with 150 m and 20 m pathlengths, respectively. The White type multi-pass gas cells shown in Fig. 1 were used to reach these long interaction distances and to increase the THz absorbances. While the FT-Far-IR rotational lines are limited by the maximal resolution of the high-resolution interferometer (around 30 MHz), the THz CH_4 lines measured by cw-THz spectroscopy are fully resolved and Doppler limited. These THz frequencies resulting from the gaussian fit of the low-pressure line profile have improved the accuracies of the ground state and the $\nu_4 \leftarrow \nu_4$ hot band molecular parameters allowing a better global modelling of the CH_4 emission and absorption used to determine the molecular abundance of this major GHG in Earth's atmosphere and also in various (exo)planetary upper atmospheres [18,26].

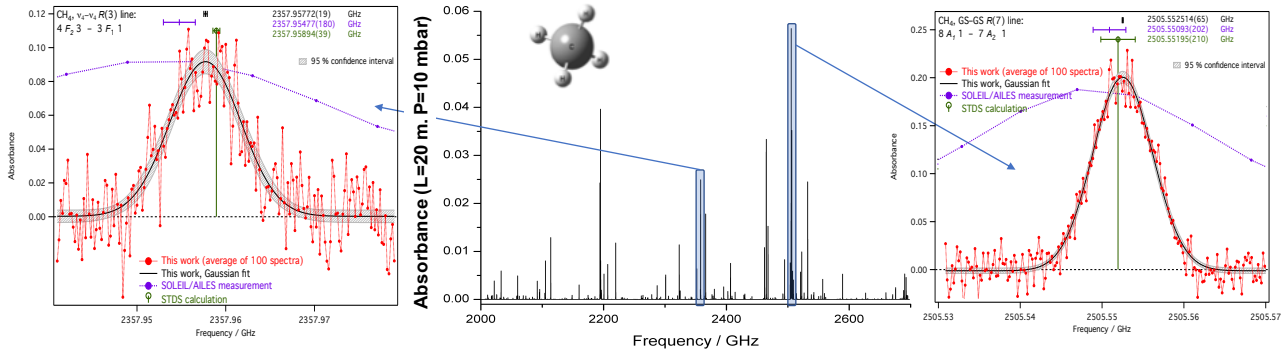

Figure 2. Central part: Absorption of ground state rotational THz lines of CH_4 induced by centrifugal distortion simulated for a pathlength of 20 m. and a pressure of 10 mbar. Left and right parts: two examples of experimental lines measured at 30 MHz resolution, $P = 10$ mbar and $L = 150$ m by FT-FIR spectroscopy using the AILES beamline of the SOLEIL synchrotron (blue solid line) and at 30 kHz resolution, $P = 1.5$ mbar and $L = 20$ m with the cw-THz photomixing spectrometer [12]. Calculations were performed using the STDS software [24], which is par of the XTDS [25] package that implements the tensorial formalism developed for spherical-top molecules in the Dijon group.

3.2. Trace gases THz measurements of N_2O and O_3 in an atmospheric simulation chamber equipped with a Chernin type multi-pass cell

A ppm LOD is required to monitor CH_4 in our atmosphere. Due to the weak intensities of pure rotational lines, THz spectroscopic monitoring of methane at atmospheric concentrations would prove serious difficulties even after a strong improvement of the spectrometers sensitivity. On the contrary, the THz trace gas detection of polar GHGs already proved its capability by the monitoring of N_2O and O_3 in the stratosphere with the MLS and TALIS sounders [8,9]. These THz heterodyne receivers are able to determine atmospheric subppm concentration profiles in the submm- and in the mm-wave domains. A possibility to get close to the detection levels of N_2O and O_3 is demonstrated in this study by performing the first THz absorption measurements in an atmospheric simulation chamber.

Compared to CH_4, rather strong rotational transitions of N_2O and O_3, with intensities around 10^{-22} cm^{-1}/(molecule cm^{-2}) [22] were probed in the submm-wave domain using versatile spectrometers based on AMC [27]. Nevertheless, with increasing wavelengths, the THz beam divergence rises and long path THz absorption experiments becomes challenging. Recently, promising results have been obtained with compact circular multi-pass cells able to refocus the beam at each internal reflection:(i) in Ref. [28], Rothbart *et al.*, using a AMC, have measured traces of acetaldehyde in methanol down to 110 ppm with an optical path of 1.9 m in the 250 GHz region; (ii) in Ref. [11], Kim *et al.*, using THz-TDS, have recorded the pure rotational spectrum of N_2O at atmospheric pressure with a dilution of 1% by reaching a THz path of 18.61 m. Even if the results of these studies are interesting since they were obtained without pre-concentration in a very compact and easily transportable gas cell, the LOD reached is clearly not sufficient for trace gas detection in the atmosphere. Yet it is possible to reach lower LOD with longer THz path-lenghts using a multi-pass cell based on the clever Chernin arrangement [29]. Compared to the White type arrangement discussed in the previous section, a Chernin multi-pass cell optimizes the recirculating of the beam over many focused lines on the field mirrors [30]. In particular longer wavelengths are very critical due to the overlapping between adjacent refocusing points within the cell what needs to be avoided or at least limited in order to prevent the presence of stationary waves yielding to baseline variations. Moreover the optical path-length in the Chernin arrangement is easy to adjust with a matrix distribution of the refocusing points and a variable number of rows and columns. As shown in Fig.3, we have dimensionned a Chernin multi-pass cell in order to integrate it in CHARME (Chamber for the Atmospheric Reactivity and the Metrology of the Environment), a 9.2 m^3, evacuable cylinder used to simulate the physical-chemistry of the atmosphere in a controlled environment [31]. The Chernin type optical setup called hereafter "MultiCHARME" is composed of 5 mirrors (2 rectangular field mirrors and 3 spherical objective mirrors) each with

177 5 m radius of curvature corresponding to the 5 m baselength of CHARME. All mirror holders are
178 equipped with computer-controlled micrometric screws for optical adjustments and path length
179 changes. MultiCHARME was designed to be coupled with different spectrometers covering a very
180 large spectral range from visible to sub-mm wavelengths.

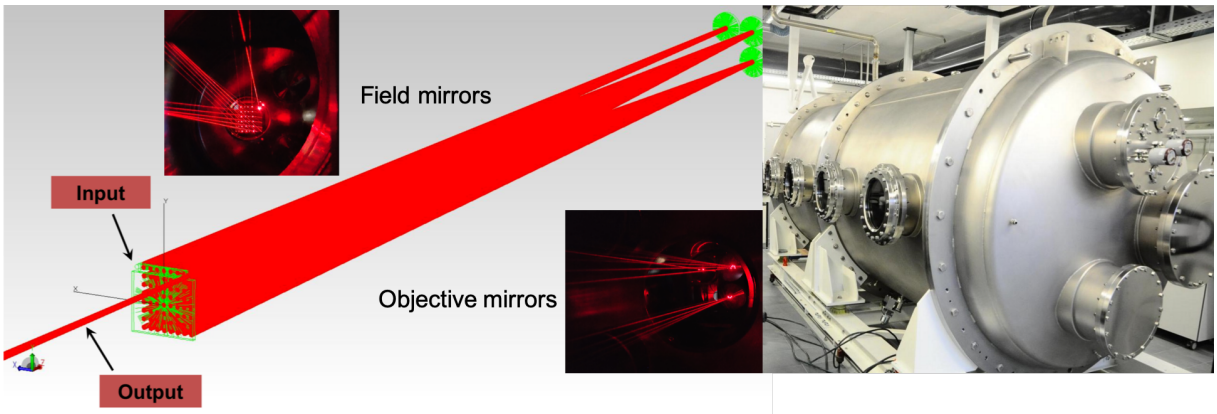

Figure 3. Left: Scheme of the MULTICHARME Chernin cell with pictures, inside CHARME, of the 6×6 arrangement highlighted with a He-Ne laser on the 2 fields and 3 objective mirrors. Right: external view of CHARME: CHamber for Atmospheric Reactivity and Metrology of the Environment located in the LPCA, Dunkirk, France.

181 N_2O was chosen as a test molecule to characterize the performances of MultiCHARME on three
182 frequency decades. In particular, the linearity of the absorption was checked with rovibrational
183 measurements up to 480 m in the near-IR and with rotational measurements up to 240 m in the THz
184 domain [32]. In Figure 4, a rotational absorbance of 32 % at 577.58 GHz (P=0.7 mbar) is obtained by
185 measuring in CHARME 400 ppm of residual N_2O traces with a THz path-length adjusted to 200 m
186 (configuration 4×5 on the field mirror). Measurements of ozone at a trace level of 200 ppm were
187 also performed in the same configuration with an absorbance of 25 % at 577.58 GHz (P=1 mbar). We
188 benefited from the possibility to simultaneously modulate the amplitude and frequency of the AMC. It
189 was of particular utility to minimise the effects of the standing waves disturbing the baseline spectra
190 measured in MultiCHARME. A rapid frequency modulation was applied with a depth corresponding
191 to the FSR of the interaction length. The absorption profiles of the targeted lines displayed a collisional
192 broadening in excess of this FSR. The profiles were measured using a significantly slower amplitude
193 modulation and a lock-in amplifier to extract the correct modulation frequency. In the right part of fig.4,
194 the absorbances of N_2O and O_3, respectively at typical tropospheric and stratospheric concentrations
195 have been simulated with HITRAN on the web [23]. Absorption levels lower than $1.0 \times 10^{-8}\ cm^{-1}$ and
196 $2.5 \times 10^{-7}\ cm^{-1}$ should be reached to measure, respectively, tropospheric N_2O and stratospheric O_3.
197 With a THz path-length of 200 m, the associated absorbances are respectively 2000 times and 50 times
198 weaker that those measured with MultiCHARME. The capability to monitor N_2O and O_3 with typical
199 atmospheric concentrations depend now on a correct modelisation of the subsisting baseline variations
200 due to long path FP effects. By removing these baseline oscillations, we can reasonably hope to reach
201 sufficient SNR to monitor O_3 in CHARME at stratospheric concentration with the same setup. The
202 measurement of tropospheric N_2O requires to improve by at least two orders of magnitude the LOD.
203 Finally, we can notice that the LOD actually reached using THz spectroscopy in MultiCHARME is
204 already sufficient to monitor N_2O collected in specific polluted atmosphere such as dental office where
205 the waste anesthetic N_2O exposure could reach several hundreds of ppm without adapted extractors
206 [33].

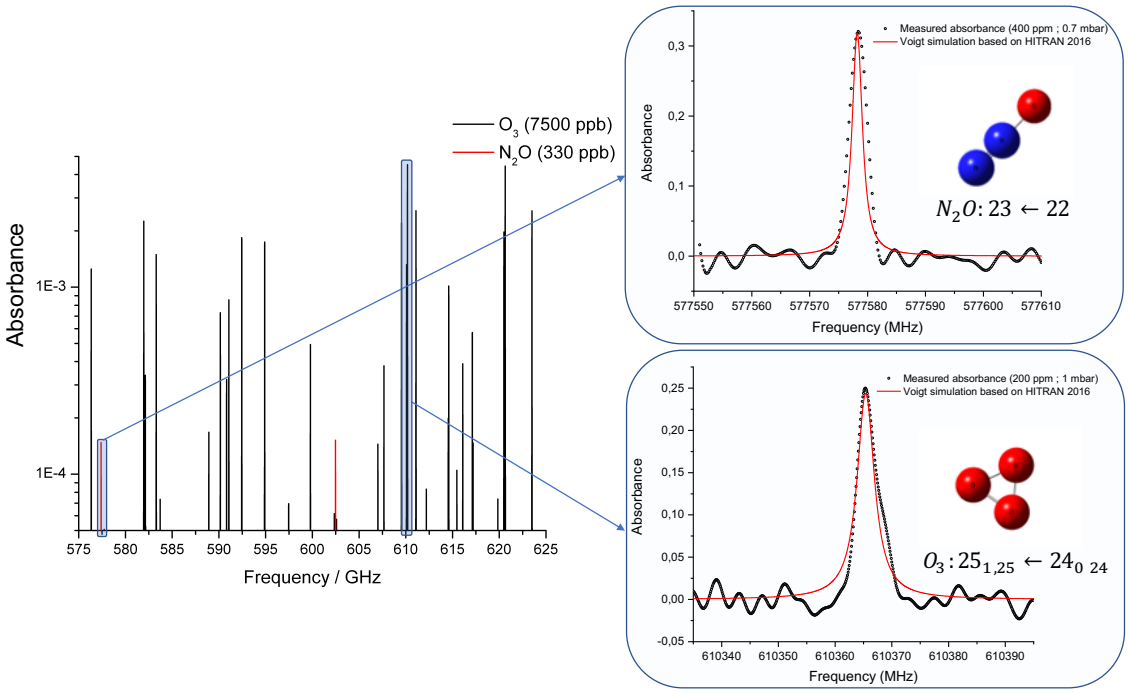

Figure 4. Left: Simulation of the rotational absorption in the 575-625 frequency region of N_2O and O_3 at tropospheric (330 ppb) and stratospheric (7.5 ppm) concentrations, respectively, for a THz pathlength of 200 m. Right: 400 ppm of N_2O at $P = 0.7$ mbar and 200 ppm of O_3 at $P = 1.0$ mbar measured in CHARME with the MultiCHARME setup in a 4×5 Chernin configuration providing a THz pathlength of 200 m (black open circles). Both lines have been measured with an amplitude modulated at 4.5 kHz. An additional frequency modulation at 50 kHz with a 1.1 MHz depth was added to limit the baseline oscillations. The red solid lines correspond to Voigt profiles simulated with HITRAN2016 tabulated frequencies, linewidths and intensities.

3.3. Intra-cavity THz measurements of CF_4

In the previous sections, we have shown that multi-pass cells provide higher sensitivity for the measurements of weak rotational resonances or small number of absorbing molecules leading to THz line with low intensities. But these cells are limited by a significant attenuation of the input THz power and generally require large volumes to reach distances exceeding 100 m. An alternative approach is to adapt the intra-cavity techniques developed in the IR domain to the longer wavelengths of the THz/submm-wave spectral domains. In 2019, our group challenges this feat by developing a THz resonator based on a low-loss oversized corrugated waveguide closed with highly reflective photonic mirrors made from silicon discs [34]. The length of the cavity is finely adjusted using piezo-electric actuators to move the mirrors by up to 250 μm, a control loop locks the cavity length to the THz frequency. With Fabry-Perot THz absorption spectroscopy (FP-TAS), we were able to perform gas phase measurements with a finesse better than 3000 in the 620 GHz frequency range. With such high-finesse, an equivalent interaction length of 1 km is estimated with a cavity of 48 cm long. It was demonstrated by measurements on a low abundant OCS isotopologue that FP-TAS is clearly able to measure transitions with intensities of about 10^{-27} cm^{-1}/(molec cm^{-2}). A scheme and a picture of the THz FP cavity is given in Fig. 5. We can notice that the quality of the cavity should be optimised and must remain stable to perform quantification. The measured signal is not directly the molecular absorption it is the second harmonic of a frequency modulated THz. It indicates the strength and width of the cavity mode as it scans across the molecular line. The absorption by the molecule causes a reduction in the signal allowing the line centre to be reliably determined and quantification undertaken for a given cavity configuration. For all these reasons, a step of calibration is still required.

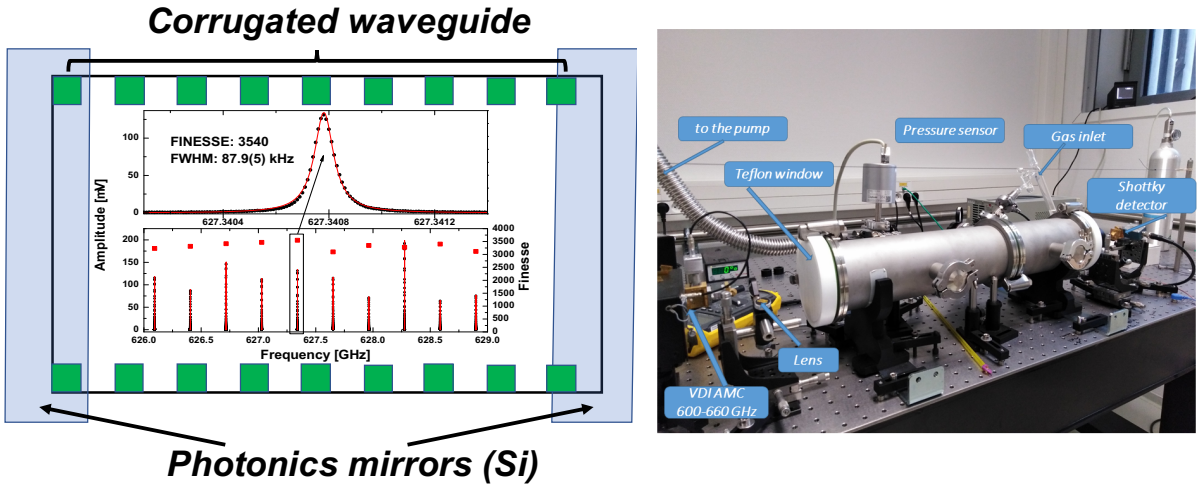

Figure 5. Left: Scheme of the Fabry-Perot THz cavity based on a low-loss oversized corrugated waveguide with highly reflective photonic mirrors. Successive cavity modes are shown inside the cavity scheme and an achieved finesse above 3500 in the 626-629 GHz frequency range is highlighted ($L_{eff.} > 1.1\ km$). Right: Picture of the FP-THz absorption spectrometer with some legends.

In the present article, we present new measurements performed with this cavity on CF_4 a very stable GHG, with a high greenhouse warming potential (> 6500) [2]. As for CH_4, CF_4 is not polar and only rotational transitions induced by centrifugal distortion or vibrational anharmonicity may be observed. Compared to CH_4, the heavier CF_4 molecule exhibits ground state pure rotational transitions at lower frequencies with a maximum intensity around 650 GHz. According to *ab initio* parameters [35], the distortion-induced dipole is estimated to only 0.324 μD. Therefore, all the THz lines are very weak with intensities never exceeding 10^{-27} cm^{-1}/(molec cm^{-2}). At room temperature, rotational transitions belonging to the hot band $v_3 = 1$ are slightly more intense compared to the ground state transitions. Rotational clusters in the R branch of this band were measured by FT-THz spectroscopy based on synchrotron source with a path-length of 150 m in the White-type cell shown in Fig. 1 (right part) [36]. In this study, the observation of CF_4 rotational clusters has required to co-add more than 5000 spectra measured at middle resolution (0.01 cm^{-1}) and pressure-broadened at P=100 mbar. Due to a lack of sensitivity and resolution, it was not possible to measure at lower pressure and to fully resolve the tetrahedral splitting of CF_4 rotational lines. Moreover, the ground state transitions with absorbances lower than 1% (Fig. 6, upper panel) were not observed. The first measurements of the tetrahedral split components of distortion-induced rotational lines of CF_4 are presented in this work with the FP-TAS measurements performed in the 625 GHz region. The middle panel of Fig. 6 targets the frequency range accessible by FP-TAS. The THz spectrum of CF_4 is simulated at a resolution of 100 kHz with fully resolved and Doppler limited rotational lines at P=100 μbar. With a 1 km path-length, absorbances above 1 % are reached for several transitions in the ground state and in the $v_3 = 1$ hot band. Finally, four examples of measured lines by FP-TAS in the $R(20)$ cluster are presented in the lower panel. The lines of the multiplet were measured individually with finesses between 2800 to 3250 and pressures between 80 μbar and 150 μbar. The frequency step was fixed to few kHz and the time constant to 200 ms. The SNR for the four lines of Fig.6 are measured between 20 to 120, which shows that the measurement of very weak THz line intensities below 10^{-28} cm^{-1}/(molec cm^{-2}) may be for now considered in THz spectroscopy. Considering this level of intensity now reachable, we can expect trace gas detection of N_2O and O_3 (Fig. 4) by FP-TAS in the THz cavity at a subppm LOD, enough for a detection at atmospheric concentrations.

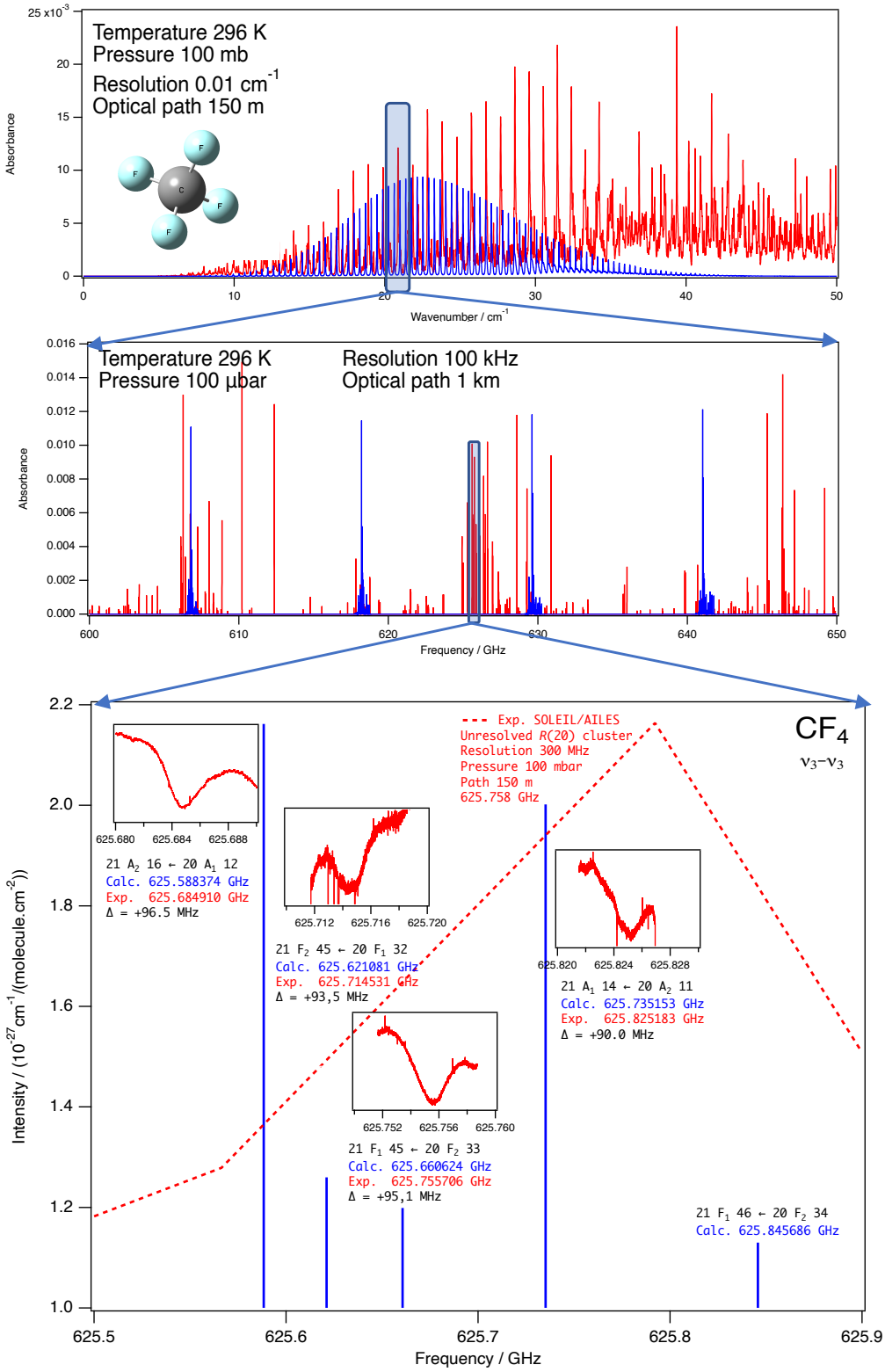

Figure 6. Upper panel: Simulation of the CF_4 THz absorbance in the conditions of the synchrotron-based FT-Far-IR measurements (see Ref.[36]), namely a resolution of 0.01 cm^{-1}, a gas pressure of 100 mbar and a path-length of 150 m. Middle panel: Simulation of the CF_4 THz absorbance measured in the frequency range accessible by FP-TAS at a resolution of 100 kHz with a gas pressure of 100 μbar and an effective path-length of 1 km. For both simulations, ground state transitions are in blue, $\nu_3 = 1$ hot band transitions are in red. Lower panel: Zoom on experimental individual rotational lines ($R(20)$ cluster in the $\nu_3 \leftarrow \nu_3$ hot band) measured by FP-TAS. The experimental THz frequencies are determined by the microwave synthesiser used to drive the amplified multiplier chain. The microwave synthesiser is referenced to a time signal provided by a GPS receiver. The calculated frequencies are determined using the STDS software [24]. Dashed red line correspond to the FT-Far-IR synchrotron based measurements at a pressure of 100 mbar and a resolution of 0.01 cm^{-1}.

4. Conclusions

The present article highlights the best performances reached by rotational submm-wave/THz long-path absorption spectroscopy of important atmospheric GHGs. The results obtained on CH_4 and CF_4 demonstrate that the weakly intense centrifugal distortion-induced rotational lines are measurable with a high degree of accuracy thanks to the progresses of THz gas phase high-resolution spectroscopy. Several percents of methane absorbances with a path-length of 20 m may be measured above 2 THz by a cw-THz photomixing source coupled to a White-type multi-pass cell. Thanks to a frequency metrology based on a frequency comb, the rotational line centers are measured with an accuracy competitive with those of electronic synthesizers and few cw-THz measurements are able to improve the ground state low-order molecular parameters of the CH_4 spherical top [12]. The study of CH_4 has been focused on THz line position analysis but absolute intensities measurements are required for quantitative spectrosocopy of methane. Such analysis requires the improvement of the spectrometer sensitivity. For this purpose, photomixers using a metallic mirror-based FP cavity could be tested at short term in order to increase significantly the power of the source [37]. Next a new generation of spectrometers has to be imagined allowing technological breakthroughs in the THz frequency gap. The use of cavity enhanced techniques initially developed in the IR hold great promise, as demonstrated by the results on CF_4 presented in this study where the tetrahedral splitting of CF_4 rotational lines have been measured and resolved by FP-TAS in the submm-wave domain. This technique based on a high finesse cavity allows to reach km effective path-length in a compact gas cell. According to the CF_4 lines measured in Fig. 6 (lower panel), FP-TAS with a finesse >3200 should be able to measure rotational lines with SNR>3 for transitions with minimal intensities up to 10^{-28} $cm^{-1}/(molec.cm^{-2})$. The results presented in this article constitute a first step of a larger study of the CF_4 pure rotational spectrum by FP-TAS: numerous lines in the 600-650 GHz frequency range (see Fig. 6, middle panel) with absorbances > 1 % have to be measured, especially the ground state lines. The measured line frequencies will be included in a global fit of the CF_4 ground state and $v_3 = 1$ molecular parameters in order to update the TFMeCaSDa database [38]. No doubt that the THz spectroscopy studies of GHGs such as CH_4 and CF_4 have to be continued. In addition, new spectroscopic data may be also obtained by considering the asymmetric isotopologues of non polar GHGs. In particular, with the high sensitivity offered by our THz cavity, it will probably possible to measure the R(27) and R(28) rotational transitions of asymmetric $^{16}O^{12}C^{18}O$ and to improve its ground state constants fitted only with low J value cm- and mm-wave transitions[39].

On the other hand, the trace gas detection of non or weakly polar GHGs at atmospheric concentration can not be seriously considered. In the case of the polar stable N_2O and unstable O_3 GHG the situation is different since we demonstrated our ability to measure these molecules at trace levels. For the first time, THz spectroscopy was used for a direct monitoring of molecular species in an atmospheric simulation chamber. Thanks to a specially designed Chernin multi-pass cell allowing to adjust a THz pathlength from 120 m to 240 m, quantitative rotational measurements of N_2O and O_3 traces were performed. Right now, the accessible detection levels for both compounds are limited to tens of ppm. We are working on a correct baseline modelisation in order to remove its variations due to multiple interfering stationary waves in the Chernin cell. Anyway, the first results obtained in CHARME with the coupling of a THz source to the MultiCHARME setup opens new possibilities especially for the monitoring of stratospheric reaction processes at low-pressure. In particular, the versatility of the electronic sources will allows to perform time-resolved quantitative spectroscopies of reactants, oxidants and products involved in targeted reactions occurring in the high altitude atmospheric layers. Moreover, it will be interesting to measure in CHARME, at different pressures, the THz self-continuum of water absorption with the AMC coupled to MultiCHARME and to compare our spectra with those recently performed with the coherent THz synchrotron radiation coupled to the White-type cell shown in Fig. 1 (right part) [40]. Finally, the high-finesse THz cavity has also to be employed for the detection of stable N_2O and unstable O_3 GHG. Next studies will

be dedicated to verify if N_2O and O_3 submm-wave transitions could be measured at tropospheric (330 ppb) and stratospheric (7500 ppb) concentrations by FP-TAS.

Author Contributions: conceptualization, A.C. and V.B.; methodology, A.C., F.H., G.M., R.B., J.D., E.F. and V.B.; software, F.H.; validation, A.C. and V.B.; investigation, C.B., J.B., J.D., E.F, A.P. and A.C.; formal analysis, C.B., J.B., J.D., A.P. and V.B.; writing–original draft preparation, A.C.; writing–review and editing, F.H., R.B., J.B. and V.B.; supervision, A.C., G.M. and F.H.; project administration, A.C., V.B. and G.M.; funding acquisition, A.C., G.M. and E.F.

Funding: This work was supported by the CaPPA project (Chemical and Physical Properties of the Atmosphere) funded by the French National Research Agency (ANR-11-LABX-0005-01) and the CLIMIBIO program supported by the Hauts-de-France Regional Council, the French Ministry of Higher Education and Research and the European Regional Development Fund. C.B. and J.D. were also funded by CLIMIBIO. The photomixing cw-THz spectrometer has been funded both by the Délégation Générale pour l'Armement (DGA, ProjetANR-11-ASTR-0035), the Institut de Recherche en Environnement Industriel (IRENI) and the European Commission via the Interreg IVA-2seas (Cleantech Project). MultiCHARME was founded by the University of Littoral and its Research Quality Bonus. The THz cavity and A.P. were funded by the Satt-Nord (project Teraspec-M0407), the French ANR (ANR-15-CE29-0017) and the European Regional Development Fund (INTERREG V FR-WA-VL 1.2.11).

Acknowledgments: We thank: (i) the AILES beamline team for the synchrotron based FT-THz experiments, especially the beamline manager P. Roy and O. Pirali in charge of the FT-FIR measurements in the White type cell; (ii) W. Zhao and B. Fang for the development of the Chernin cell; (iii) C. Coeur, N. Houzel and P. Kulinski for their assistance during the measurements in the CHARME chamber.

Conflicts of Interest: The authors declare no conflict of interest.

Abbreviations

The following abbreviations are used in this manuscript:

ACE	Atmospheric Chemistry Experiment
AILES	Advanced Infrared beamLine Exploited for Spectroscopy
AMC	Amplified Multiplier Chains
CFCs/HCFCs	ChloroFluoroCarbons
CHARME	CHamber for the Atmospheric Reactivity and the Metrology of the Environment
cw-THz	continuous-wave Terahertz
FFT	Fast Fourier Transform
FP-TAS	Fabry-Perot Terahertz Absorption Spectroscopy
FSR	Free Spectral Range
FTS	Fourier Transform Spectrometer
GHG	Greenhouse gas
HITRAN	HIgh-resolution TRANsmission molecular absorption database
IASI	Infrared Atmospheric Sounding Interferometer
IR	InfraRed
LOD	Level of Detection
LTG-AsGa	Low-Temperature Grown - Arsenide Gallium
MLS	Microwave Limb Sounder
NEP	Noise Equivalent Power
SCISAT	SCIence Satellite
SNR	Signal to Noise Ratio
SOLEIL	Source Optimisée de Lumière d'Énergie Intermédiaire du LURE
STDS	Spherical-Top Data System
TALIS	THz Atmospheric Limb Sounder
TES	Tropospheric Emission Spectrometer
TFMeCaSDa	TetraFluoroMethane Calculated Spectroscopic Databases
THz-TDS	Terahertz-Time Domain Spectroscopy
LO	Local Oscillator
UV	Ultraviolet
ZBD	Zero Bias Detector

References

1. U.S. Environmental Protection Agency, Global Greenhouse Gas Emissions Data". U.S. Environmental Protection Agency. Retrieved 30 December 2019. The burning of coal, natural gas, and oil for electricity and heat is the largest single source of global greenhouse gas emissions. In *Global Greenhouse Gas Emission Data*, retrieved 30 Nov. 2019.
2. Ravishankara, A. R., Solomon S., Turnipseed A. A. and Warren R. F.: Atmospheric lifetimes of long-lived halogenated species. *Science* **1993**, *259*,194-199.
3. Butler, J. and Montzka S., The NOAA Annual Greenhouse Gas Index (AGGI). NOAA Global Monitoring Laboratory/Earth System Research Laboratories, 14 August 2020.
4. Myhre, G., D. Shindell, F.-M. Bréon, W. Collins, J. Fuglestvedt, J. Huang, D. Koch, J.-F. Lamarque, D. Lee, B. Mendoza, T. Nakajima, A. Robock, G. Stephens, T. Takemura and H. Zhang, 2013: Anthropogenic and Natural Radiative Forcing. In: Climate Change 2013: The Physical Science Basis. Contribution of Working Group I to the Fifth Assessment Report of the Intergovernmental Panel on Climate Change [Stocker, T.F., D. Qin, G.-K. Plattner, M. Tignor, S.K. Allen, J. Boschung, A. Nauels, Y. Xia, V. Bex and P.M. Midgley (eds.)]. Cambridge University Press, Cambridge, United Kingdom and New York, NY, USA.
5. Clerbaux, C., Boynard, A., Clarisse, L., George, M., Hadji-Lazaro, J., Herbin, H., Hurtmans, D., Pommier, M., Razavi, A., Turquety, S., Wespes, C., and Coheur, P.-F.: Monitoring of atmospheric composition using the thermal infrared IASI/MetOp sounder. *Atmos. Chem. Phys.* **2009**, *9*, 6041–6054.
6. Bernath, P.-F.: The Atmospheric Chemistry Experiment (ACE). *J. Quant. Spectrosc. Radiat. Transf.* **2017**, *186*, 3-16.
7. Beer, R.: TES on the Aura Mission: Scientific Objectives, Measurements, and Analysis Overview. *IEEE Trans. Geosci. Remote Sensing* **2006**, *44(5)*, 1102–1105.
8. Froidevaux, L., Livesey, N. J., Read, W. G., Jiang, Y. B., Jimenez, C., Filipiak, M. J., ...Hendershot, R.: Early validation analyses of atmospheric profiles from EOS MLS on the aura Satellite. *IEEE Trans. Geosci. Remote Sensing* **2006**, *44(5)*, 1106–1121.
9. Wang, W., Wang, Z., Duan, Y.: Performance evaluation of THz Atmospheric Limb Sounder (TALIS) of China. *Atmos. Meas. Tech.* **2020**, *13*, 13-38.
10. Tran, H., Cuisset, A., Payan, S., Schwell, M., Té, Y., Tomasini, L., Giraud-Héraud, Y.: The first Vietnam School of Earth Observation: Atmospheric Remote Sensing and Molecular Spectroscopy. *Vietnam J. of Earth Sciences* **2019**, *41*, 138-155.
11. Kim, G.-R.; Lee, H.-B., Jeon, T.-I.: Terahertz Time-Domain Spectroscopy of Low Concentration N_2O using Long-Range multi-pass Gas Cell. *IEEE Trans. THz Sci. Technol.* **2020**, *10(5)*, 524-530.
12. Bray, C., Cuisset, A., Hindle, F., Mouret, G., Bocquet, R., Boudon, V.: Spectral lines of methane measured up to 2.6 THz at sub-MHz accuracy with a cw-THz photomixing spectrometer: Line positions of rotational transitions induced by centrifugal distortion. *J. Quant. Spectrosc. Radiat. Transf.* **2017**, *203*, 349-354.
13. Hindle, F., Mouret, G., Eliet, S., Guinet, M., Cuisset, A.,Bocquet, R., Yasui, T., Rovera, D.: Widely tunable THz synthesizer. *Appl. Phys. B* **2011**, *104*, 763-769.
14. White, J. U.: Long optical paths of large aperture. *J. Opt. Soc. Amer.* **1942**, *32(32)*, 285-288.
15. Podobedov, V.-B., Plusquellic, D.-F, Fraser, G.-T.: Investigation of the water-vapor continuum in the THz region using a multi-pass cell. *J. Quant. Spectrosc. Radiat. Transf.* **2005**, *91*, 287-295.
16. Winnewisser, M., Winnewisser, B.-P, Stein, M., Birk, M., Wagner, G., Winnewisser, G., Yamada, K., Belov, S.-P., Baskakov, O.-I.: Rotational Spectra of cis-HCOOH, trans-HCOOH, and trans-H^{13}COOH. *J. Mol. Spectrosc.* **2002**, *216*, 216, 259–265.
17. Brubach, J.-B., Manceron L., Rouzières M., Pirali O., Balcon D., Tchana F., Boudon V., Tudorie M., Huet T., Cuisset A., Roy P.: Performance of the AILES THz-infrared beamline on SOLEIL for high resolution spectroscopy. *AIP Conf. Proc.* **2010**, *1214*, 81-84.
18. Boudon V., Pirali O., Roy P., Brubach J.-B., Manceron L., Auwera J.-V.: The high- resolution far-infrared spectrum of methane at the SOLEIL synchrotron. *J. Quant. Spectrosc. Radiat. Transf.* **2010**, *111*, 1117-1129.
19. Sanzharov M., Auwera J.-V., Pirali O., Roy P., Brubach J.-B., Manceron L., Gabard T., Boudon V.: Self and N_2 collisional broadening of far-infrared methane lines measured at the SOLEIL synchrotron. *J. Quant. Spectrosc. Radiat. Transf.* **2012**, *113*, 1874-1886.

20. Harmon, S.-A., Cheville, R.-A.: Part-per-million gas detection from long-baseline THz spectroscopy. *Appl. Phys. Lett.* **2004**, *85*, 2128-2130.
21. Hindle, F.,Yang, C., Mouret, G., Cuisset, A., Bocquet, R., Lampin, J.-F., Blary, K., Peytavit, E., Akalin, T. and Ducournau, G.: Recent Developments of an Opto-Electronic THz Spectrometer for High-Resolution Spectroscopy. *Sensors* **2009**, *9*, 9039-9057.
22. Gordon, I.-E.,Rothman, L.-S.,Hill, C. *et al.*, : The HITRAN2016 Molecular Spectroscopic Database. *J. Quant. Spectrosc. Radiat. Transf.* **2017**, *203*, 3-69.
23. https://hitran.iao.ru
24. Wenger C., Champion J.P.: Spherical top data system (STDS) software for the simulation of spherical top spectra. *J. Quant. Spectrosc. Radiat. Transf.* **1998**, *59*, 471-480.
25. Wenger C., Boudon V., Rotger M., Sanzharov J.P. and Champion J.P.: XTDS and SPVIEW: graphical tools for the analysis and simulation *J. Mol. Spectrosc.* **2008**, *251(1-2)*, 102-113.
26. Amyay, B., Gardez, A., Georges, R., Biennier, L., Vander Auwera, J., Richard, C., Boudon, V.: New investigation of the ν_3 C–H stretching region of $^{12}CH_4$ through the analysis of high temperature infrared emission spectra. *J. Chem. Phys.* **2018**, *148*, 134306.
27. Mouret, G., Guinet, M., Cuisset, A., Croize, L., Eliet, S., Bocquet, R., Hindle, F.: Versatile Sub-THz Spectrometer for Trace Gas Analysis. *IEEE Sensors J.* **2013**, *13(1)*, 133-138.
28. Rothbart, N., Schmaltz K., Hübers, H.-W.: A Compact Circular multi-pass Cell for Millimeter-Wave/Terahertz Gas Spectroscopy. *IEEE Trans. THz Sci. Technol.* **2019**, *10(1)*, 8884743, 9-14.
29. Chernin, S.-M.: New generation of multi-pass systems in high resolution spectroscopy. *Spectrochim. Acta, Part A* **1996**, *52*;, 1009-1022.
30. Tchana, F. K., Willaert, F., Landsheere, X., Flaud, J.-M., Lago, L., Chapuis, M., Herbeaux, C., Roy, P., Manceron, L.: A new, low temperature long-pass cell for mid-infrared to terahertz spectroscopy and synchrotron radiation use. *Rev. Sci. Instrum.* **2013**, *84*, 093101.
31. Meng, L., Coeur, C., Fayad, L., Houzel, N., Genevray, P., Bouzidi, H., Tomas, A., Chen, W.: Secondary organic aerosol formation from the gas-phase reaction of guaiacol (2-methoxyphenol) with NO_3 radicals. *J. Atmos. Env.* **2020**, *240*, 1117740.
32. Decker, J. *et al.*: MULTICHARME: a Chernin type multi-pass cell designed for IR and THz spectroscopies experiments in CHARME *manuscript in progress*, **2021**
33. Deng, H.-B., Li, F.-X., Cai, Y.-H., Xu, S.-Y.: Waste anesthetic gas exposure and strategies for solution. *J. Anesthes.* **2018**, *32*, 269-282.
34. Hindle, F., Bocquet, R., Pienkina, A., Cuisset, A., Mouret, G.: Terahertz gas phase spectroscopy using a high-finesse Fabry–Pérot cavity. *Optica*, **2019**, *6(12)*, 1449-1454.
35. Rey, M., Chizhmakova, I.-S., Nikitin, A.-V., Tyuterev, V.-G.: Understanding global infrared opacity and hot bands of greenhouse molecules with low vibrational modes from first-principles calculations: the case of CF_4. *Phys. Chem. Chem. Phys.*, **2018**, *20*, 21008-21033.
36. Boudon, V., Carlos, M., Richard C., Pirali, O.: Pure rotation spectrum of CF_4 in the $v_3 = 1$ state using THz synchrotron radiation. *J. Mol. Spectrosc.*, **2018**, *348*, 43-46.
37. Peytavit, E., Latzel, P., Pavanello, F., Ducournau, G., Lampin J.-F.: CW source based on photomixing with output power reaching 1.8 mW at 250 GHz. *IEEE Electron. Device Lett.*, **2013**, *34*, 1277–1279.
38. Richard, C., Boudon, V. and Rotger, M.: Calculated spectroscopic databases for the VAMDC portal: New molecules and improvements. *J. Quant. Spectrosc. Radiat. Transfer*, **2020**, *251*, 107096.
39. Endo, Y., Yoshida, K., Saito, S., Horota, E.: The microwave spectrum of carbon dioxide - ^{18}O. *J. Chem. Phys.*, **1980**, *73*, 3511-3512.
40. Odintsova, T.-A., Tretyakov, M.-Y., Zibarova, A.-O., Pirali, O., Roy, P., Campargue A.: Far-infrared self-continuum absorption of $H_2^{16}O$ and $H_2^{18}O$ (15–50 cm^{-1}). *J. Quant. Spectrosc. Radiat. Transfer*, **2019**, *227*, 190-200.